Pseudo-Streaming Potentials in *Necturus* Gallbladder Epithelium

I. Paracellular Origin of the Transepithelial Voltage Changes

LUIS REUSS, BRUCE SIMON, and ZHIJIAN XI

From the Department of Physiology and Biophysics, University of Texas Medical Branch, Galveston, Texas 77550

ABSTRACT   Apparent streaming potentials were elicited across *Necturus* gallbladder epithelium by addition or removal of sucrose from the apical bathing solution. In NaCl Ringer's solution, the transepithelial voltage (V_{ms}) change (reference, basolateral solution) was positive with sucrose addition and negative with sucrose removal. Bilateral Cl^- removal (cyclamate replacement) had no effect on the polarity or magnitude of the V_{ms} change elicited by addition of 100 mM sucrose. In contrast, bilateral Na^+ removal (tetramethylammonium [TMA^+] replacement) inverted the V_{ms} change (from 2.7 ± 0.3 to -3.2 ± 0.2 mV). Replacement of Na^+ and Cl^- with TMA^+ and cyclamate, respectively, abolished the change in V_{ms}. Measurements of cell membrane voltages and relative resistances during osmotic challenges indicate that changes in cell membrane parameters do not explain the transepithelial voltage changes. The initial changes in V_{ms} were slower than expected from concomitant estimates of the time course of sucrose concentration (and hence osmolality) at the membrane surface. Paired recordings of the time courses of paracellular bi-ionic potentials (partial substitution of apical Na^+ with tetrabutylammonium [TBA^+]) revealed much faster time courses than those produced by sucrose addition, although the diffusion coefficients of sucrose and TBACl are similar. Hyperosmotic and hypoosmotic challenges yielded initial V_{ms} changes at the same rate; thereafter, the voltage increased with hypoosmotic solution and decreased with hyperosmotic solution. These late voltage changes appear to result from changes in width of the lateral intercellular spaces. The early time courses of the V_{ms} changes produced by osmotic challenge are inconsistent with the expectations for water–ion flux coupling in the junctions. We propose that they are pseudo-streaming potentials, i.e., junctional diffusion potentials caused by salt concentration changes in the lateral intercellular spaces secondary to osmotic water flow.

INTRODUCTION

The pathways and mechanisms of transepithelial water transport across so-called leaky epithelia have been the subject of considerable study (Sackin and Boulpaep,

1975; Diamond, 1979; Hill, 1980; Weinstein, Stephenson, and Spring, 1981; Berry, 1983; Reuss and Cotton, 1988; Whittembury and Carpi-Medina, 1988; Tripathi and Boulpaep, 1989; Verkman, 1989; Schafer, 1990; Spring, 1991; Whittembury and Reuss, 1991). It is generally accepted that spontaneous fluid absorption in this class of epithelia occurs by "osmotic coupling" of water transport to active salt transport. Salt transport generates differences in osmolality across the critical epithelial barriers, and water flows in the same direction because of those differences in osmolality and the finite osmotic water permeability of the barriers. Although the osmotic theory is favored by most investigators, other mechanisms of coupling between salt and water transport have been proposed (Hill, 1975a, b; Mollgard and Rostgaard, 1978), but their experimental support is questionable (Reuss and Cotton, 1988; Whittembury and Reuss, 1991). A second issue pertains to the pathway(s) across which water is transported. In principle, water could flow across the cells and/or the paracellular pathway; i.e., the junctional complexes in series with the lateral intercellular spaces. The surface of junctional network per unit area of epithelium is very small relative to that of the cell membranes (Spring, 1991). However, the high ionic permeability of the junctions in this class of epithelia (Frömter, 1972; Guggino, Windhager, Boulpaep, and Giebisch, 1982) suggests the possibility that their osmotic water permeability is also high, and hence junctional osmotic water flow cannot be ruled out a priori.

Recent studies in proximal renal tubules (reviewed in Reuss and Cotton, 1988 and Whittembury and Reuss, 1991) and amphibian gallbladder (Persson and Spring, 1982; Cotton, Weinstein, and Reuss, 1989) have demonstrated that both apical and basolateral cell membranes have high osmotic water permeabilities, indicating that a large moiety of transepithelial osmotic water flow may be transcellular. However, these studies do not rule out the possibility of a parallel (paracellular) water flow. There are no established methods to directly assess water permeation via the junctions or to directly measure the osmotic water permeability of these structures. For this reason, arguments for or against paracellular water transport are indirect.

One of these arguments is based on the experimental observation of solute–solvent flux coupling. It is reasoned that if paracellular water permeation were via aqueous junctional pores, large enough to allow for ion and small nonelectrolyte permeation, then the water flux will be accompanied by a solute flux in the same direction (House, 1974; Hill and Hill, 1978a, b; Whittembury, de Martínez, Paz-Aliaga, and Linares, 1981). In contrast, water transport across the cell membranes is likely to occur via the lipid bilayer and/or small pores (Meyer and Verkman, 1987; Whittembury and Carpi-Medina, 1988), and hence coupling of solute and water fluxes is unlikely to occur if osmotic water flow is exclusively transcellular.

Solute–solvent coupling in leaky epithelia has been assessed by measurements of solvent drag (Hill and Hill, 1978a; Whittembury et al., 1981) and electrokinetic phenomena, in particular streaming potentials (Pidot and Diamond, 1964; Diamond and Harrison, 1966; Frömter and Gessner, 1974; De Mello, Lopes, and Malnic, 1976; Corman, 1985; Tripathi and Boulpaep, 1988). Streaming potentials can be generated across ion-selective pores or slits by imposing osmotic gradients across the pathway and measuring the resulting change in transmembrane voltage. The voltage change is due to the fact that the water flow, driven by the osmotic gradient, is

frictionally coupled to an ion flux in the same direction. Because the pores or slits are ion selective, they contain a solution with an excess of the more permeant species (either cation or anion), and hence the water-coupled ion flux results in transmembrane current flow or in a change in membrane voltage (House, 1974; Finkelstein, 1987; Tripathi and Boulpaep, 1988). A complication in the interpretation of such an experiment is that water and (selective) ion permeation via separate pathways would also be expected to cause a change in membrane voltage (Diamond, 1979; Barry and Diamond, 1984; Barry, 1989). This phenomenon, called a pseudo-streaming potential, is the result of the unavoidable presence of anatomic or hydrodynamic unstirred fluid layers in series with the permeation pathway: water flow causes an increase in salt concentration on the side from which the water flows and a decrease in salt concentration on the opposite side of the membrane, and the salt concentration gradient causes in turn a transmembrane diffusion potential across any parallel ion-selective pathway. Hence, the demonstration of a change in transepithelial voltage in response to a unilateral change in osmolarity ("apparent streaming potential") is not necessarily an indication of coupling of ion and water fluxes in a common pathway and therefore cannot be construed as an argument for paracellular water flow.

The experiments described in this and the accompanying paper were designed to test whether apparent streaming potentials can be elicited in *Necturus* gallbladder epithelium, a prototypical leaky epithelium (Frömter, 1972; Reuss and Finn, 1975a, b; Reuss, 1989), and to establish: (a) whether the voltage changes are of paracellular origin, and (b) whether the mechanism involved corresponds to that of a "true" or a "pseudo" streaming potential. The first question is addressed in this paper, and the second one in the accompanying paper (Reuss, Simon, and Cotton, 1992).

MATERIALS AND METHODS

Tissues and Solutions

Specimens of *Necturus maculosus* were maintained in aquaria at 5–10°C. The animals were anesthetized by immersion in a 1 g/liter solution of tricaine methanesulfonate. The gallbladders were removed, opened longitudinally, rinsed free of bile, and mounted apical side up in a modified Ussing chamber (Cotton and Reuss, 1989). The apical surface of the tissue was superfused by gravity, and the basolateral surface by a siphon system. The positions of superfusion and suction pipettes and measuring electrodes, as well as the volume and rate of replacement of the apical bathing solution, were maintained constant during the experiment, and reproduced from experiment to experiment (Cotton and Reuss, 1989). All experiments were carried out under microscopic observation, with the chamber positioned horizontally on the stage of an inverted microscope (Diavert; E. Leitz, Inc., Rockleigh, NJ), in turn positioned on a vibration-isolation table (Technical Manufacturing Corp., Peabody, MA).

The control bathing solution (NaCl Ringer's solution) had the following composition (mM): 90 NaCl, 10 NaHCO$_3$, 2.5 KCl, 1.8 CaCl$_2$, 1.0 MgCl$_2$, and 0.5 NaH$_2$PO$_4$, and was equilibrated with 1% CO$_2$/99% air. The pH was ~7.65 and the osmolality ~200 mosmol/kg. Changes in osmolality were achieved by adding sucrose to final nominal concentrations ranging from 50 to 200 mM. In some experiments, Na$^+$ was replaced totally or partially with tetramethylammonium (TMA$^+$) or tetrabutylammonium (TBA$^+$), and/or Cl$^-$ with cyclamate. These substitutions

were mole-by-mole. The osmolalities of all solutions were measured with a vapor pressure osmometer (model 5100B; Wescor Inc., Logan, UT).

In some experiments, 50 mM NaCl was replaced with 100 mM sucrose in both apical and basolateral bathing solutions. Changes in apical solution osmolality were then obtained by removing or adding sucrose, keeping the nominal ion concentrations unchanged.

Electrical Measurements

The transepithelial voltage (V_{ms}) was measured as the difference between the electrical potentials recorded between a grounded Ag-AgCl pellet connected to the basolateral bathing solution with a short Ringer/agar bridge, and a calomel half-cell in series with a flowing, saturated-KCl bridge constructed from a fiber-filled glass pipette (Ultrawick; World Precision Instruments, Sarasota, FL), in contact with the apical bathing solution. At the high rates of superfusion used, the flowing bridge does not cause significant changes in apical solution $[K^+]$.

Membrane voltages (apical, V_{mc}; basolateral, V_{cs}) were measured with glass microelectrodes filled with 1 or 3 M KCl. The microelectrodes were pulled from borosilicate glass tubing with internal fiber (1 mm o.d., 0.5 mm i.d.; Glass Company of America, Millville, NJ), with a Brown-Flaming microprocessor-controlled puller (model P87; Sutter Instrument Co., Novato, CA) or a Narishige PD-5 puller (Narishige, Tokyo, Japan). The electrical resistances of microelectrodes filled with 3 M KCl and immersed in NaCl Ringer's solution ranged from 30 to 60 MΩ.

Cell impalements were carried out from the apical surface of the tissue, advancing the microelectrode at a 45° angle with respect to the horizontal with a hydraulic micromanipulator (MO-103; Narishige). Impalement validation was as described before (Weinman and Reuss, 1984; Altenberg, Copello, Cotton, Dawson, Segal, Wehner, and Reuss, 1990).

Transepithelial constant-current pulses (i_t, usually 50 μA/cm², 1-s duration) were passed between an Ag-AgCl pellet in the basolateral compartment and an Ag-AgCl wire in the apical compartment. The resulting voltage deflections across the tissue or the individual cell membranes were corrected for series resistances and used to calculate the transepithelial resistance $(R_t = \Delta V_{ms}/i_t)$ and the apparent fractional resistance of the apical cell membrane $(R_a/(R_a + R_{bl}) = \Delta V_{mc}/\Delta V_{ms})$.

Electrical data were amplified, digitized at a rate of 10 Hz and stored for later analysis with a laboratory computer (ASYST; Macmillan Software Co., New York, NY).

Ion-selective Microelectrodes

The time course of changes in the concentration of TBA^+ near the apical surface of the epithelium was measured with a K^+-selective microelectrode referenced to the apical flowing junction electrode, as described before (Cotton and Reuss, 1989). This technique allowed us to assess the time course of the change in cation concentration at the cell surface when Na^+ was replaced with TBA^+ and also to estimate the time course of changes in sucrose concentration when sucrose was added to or removed from the bathing medium. To this end, NaCl Ringer's and sucrose-containing solutions contained TBA^+ at concentrations proportional to their osmolalities (e.g., NaCl-Ringer's solution, 1 mM TBA^+; NaCl Ringer's plus 100 mM sucrose, 2 mM TBA^+). The microelectrode is $\sim 10^6$-fold more sensitive to TBA^+ than to K^+ (Cotton and Reuss, 1989), and therefore senses the concentration of the former ion without significant interference.

Data Analysis

Results are given as means ± standard error; statistical comparisons were made by Student's t test applied to paired data. A value of $P < 0.05$ was considered significant.

RESULTS

Characteristics of the Transepithelial Voltage Changes Elicited by Increasing the Osmolality of the Apical Bathing Solution

Fig. 1 illustrates the effects of raising the osmolality of the apical bathing solution (addition of sucrose) on the transepithelial voltage (V_{ms}) and the voltage output of a TBA$^+$-selective microelectrode positioned within 3 μm of the surface of the epithelium (V_{TBA}). V_{TBA} is proportional to the log of the change in osmolality at the apical surface. Addition of sucrose to the apical bathing solution causes mucosa-positive changes in V_{ms} that develop slowly (relative to the changes in osmolality), reach a maximum, and in most instances decrease over 1–5 min to plateau levels. Upon returning to NaCl-Ringer's, V_{ms} returns slowly (relative to the change in osmolality) to control levels.
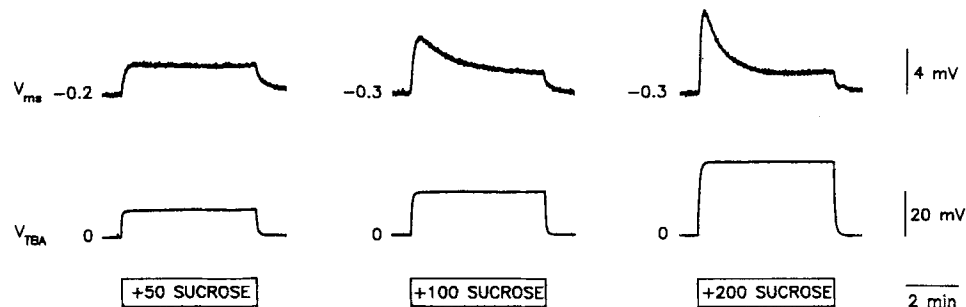

FIGURE 1. Changes in transepithelial voltage (V_{ms}) and in the difference between the voltage outputs of a TBA$^+$-sensitive microelectrode (positioned near the apical surface of the epithelium) and the apical bathing solution electrode (V_{TBA}). Sucrose was added to the apical bathing solution at the nominal concentrations (millimolar) and for the periods indicated by the bars. The changes in V_{ms} are slower than those of V_{TBA}: half-times for V_{ms} and V_{TBA} were 4.7 and 1.8, 5.1 and 2.0, and 5.1 and 2.2 s for additions of 50, 100, and 200 mM sucrose, respectively. Note that at the three sucrose concentrations tested the change in V_{ms} is in the apical solution-positive direction. V_{ms} reaches a maximum and then decreases slowly.

The time course of the V_{ms} change was clearly dependent on the magnitude of the change in osmolality, as illustrated in Fig. 1; with higher osmotic gradients there was a monotonic reduction in the voltage after a maximum positive value. The mechanism of this "decline" in the voltage with large increases in apical solution osmolality will be addressed below. Transepithelial voltage changes upon addition of 50, 100, and 200 mM sucrose to the mucosal solution are summarized in Table I.

Ion Dependence of the Transepithelial Voltage Changes

The observations presented above are consistent with an apparent streaming potential due to cation selectivity of the junctional complexes. Inasmuch as the junctions of this epithelium have a higher permeability for Na$^+$ than for Cl$^-$, either junctional water–ion flux coupling in the basolateral-to-apical direction (true streaming potential) or a transepithelial salt concentration difference due to increased concentration

TABLE I

Effects of Increases in Mucosal Solution Osmolality on Transepithelial Voltage

[Sucrose]	Transepithelial voltage				
	Control	Peak	1 min	2 min	Control
mM		mV			
+50	0.1 ± 0.3	2.9 ± 0.3*	2.8 ± 0.3*	2.1 ± 0.9*	0.3 ± 0.3
+100	0.2 ± 0.2	4.9 ± 0.4*	4.1 ± 0.6*	2.6 ± 0.3*	0.3 ± 0.2
+200	0.0 ± 0.4	7.7 ± 0.9*	5.2 ± 1.3*	2.2 ± 0.1*	−0.2 ± 0.4

Data are means ± SEM of n = 8 paired experiments. The apical solution sucrose concentration (millimolar) is given in the first column. Exposure to sucrose-containing solution lasted 2 min. Post-control values were measured 5 min after returning to the standard Ringer's solution.
*Significantly different from control (P < 0.05).

in the lateral space secondary to the water flux (pseudo-streaming potential) would account for the polarity of the observed change in transepithelial voltage.

If the above interpretation is correct, then the voltage change should be considerably attenuated, or disappear, if Na^+ is replaced in both solutions with a less-permeant cation. To test this possibility, we carried out complete replacement of Na^+ with TMA^+ in both apical and basolateral bathing solutions, and then replaced the apical solution with one having a higher osmolality (addition of 100 mM sucrose). As illustrated in Fig. 2 and summarized in Table II, the transepithelial voltage change was reversed by Na^+ removal. Inasmuch as the relative junctional Na^+ permeability is high, the relative Cl^- permeability must be low. Confirming this view, when Cl^- was replaced with cyclamate in both apical and basolateral bathing solutions, increasing the osmolality of the apical bathing solution caused a voltage change similar to that
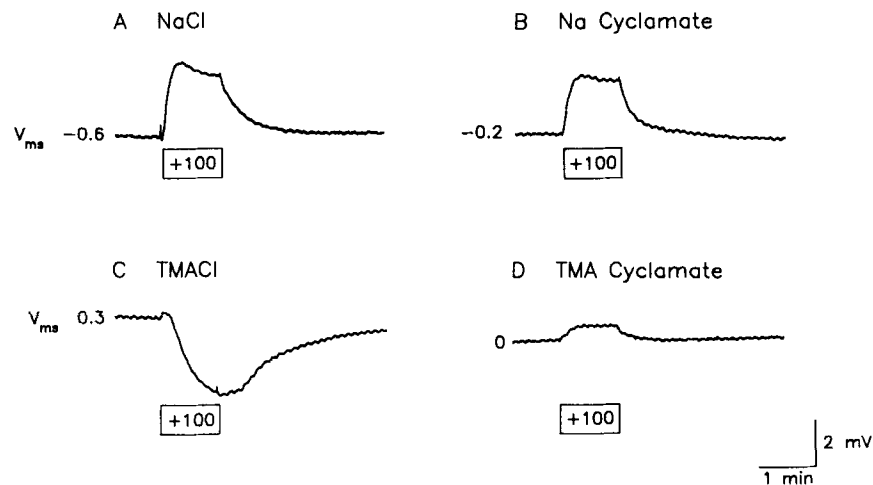

FIGURE 2. Effect of addition of 100 mM sucrose (bars) on V_{ms} during bilateral exposure to NaCl (A), Na cyclamate (Cl-free solutions) (B), TMACl (Na-free solutions) (C), and TMA cyclamate (NaCl-free solutions) (D). Note the reversal of the V_{ms} change in C and the small change in D. See text.

produced by the addition of the same sucrose concentration to NaCl Ringer's solution (Fig. 2, Table II). In principle, one could expect a larger change in Na cyclamate solution vs. NaCl solution if $P_{Cl} > P_{cycl}$. However, upon removal of Cl^-, fluid transport decreases and the lateral intercellular space tends to collapse, which by itself reduces the apparent paracellular selectivity (see Discussion).

Finally, when both Na^+ and Cl^- were replaced with TMA^+ and cyclamate, respectively, the transepithelial voltage change upon elevating mucosal osmolality was very small, suggesting similar (and low, since Na^+ replacement by TMA^+ reverses the response) junctional permeabilities for both TMA^+ and cyclamate (Fig. 2, Table II).

Changes in Transepithelial Voltage Elicited by Reducing the Apical Solution Osmolality

If the voltage changes described above are in fact apparent paracellular streaming potentials, then reducing the osmolality of the apical bathing solution should also cause changes in transepithelial voltage, but these should be opposite in polarity to

TABLE II

Effects of Na^+, Cl^-, or NaCl Removal on the Transepithelial Voltage Changes Produced by Apical Addition of 100 mM Sucrose

Bathing solution	Transepithelial voltage			
	Control	Peak	1 min	Control
			mV		
NaCl	0.3 ± 0.2	3.0 ± 0.6*	2.7 ± 0.6*	0.3 ± 0.2
TMA Cl	0.2 ± 0.2	−3.4 ± 0.1*	−3.4 ± 0.1*	0.0 ± 0.3
Na cyclamate	0.0 ± 0.2	2.6 ± 0.3*	2.5 ± 0.3*	0.1 ± 0.2
TMA cyclamate	0.1 ± 0.1	−0.3 ± 0.7	−0.3 ± 0.7	0.0 ± 0.2

Data are means ± SEM of $n = 4$ paired experiments. Na^+ replaced with TMA^+; Cl^- replaced with cyclamate. Post-control values were measured 5 min after returning to the standard Ringer's solution.
*Significantly different from control ($P < 0.05$).

those elicited by apical solution hyperosmolality. Fig. 3 compares the effects of reducing or increasing apical solution sucrose concentration on the transepithelial voltage. The tissue was initially exposed to bathing solutions in which 50 mM NaCl had been replaced with 100 mM sucrose; consequent changes in osmolality were obtained by sucrose removal or addition. A reduction in apical solution sucrose concentration produced a mucosa-negative change in transepithelial voltage which was similar in magnitude to the mucosa-positive change elicited by an increase in osmolality (Table III). However, after the initial changes, V_{ms} decreases with hyperosmotic challenge and increases with hypoosmotic challenge (Fig. 3). These slow changes in voltage are due to changes in the paracellular ion selectivity during the osmotic challenge (see below).

Lack of Contribution of Cell–Membrane Electrical Parameters to the Transepithelial Voltage Changes

The tentative conclusion that the changes in transepithelial voltage produced by changes in apical solution osmolality are of paracellular origin implies that there is
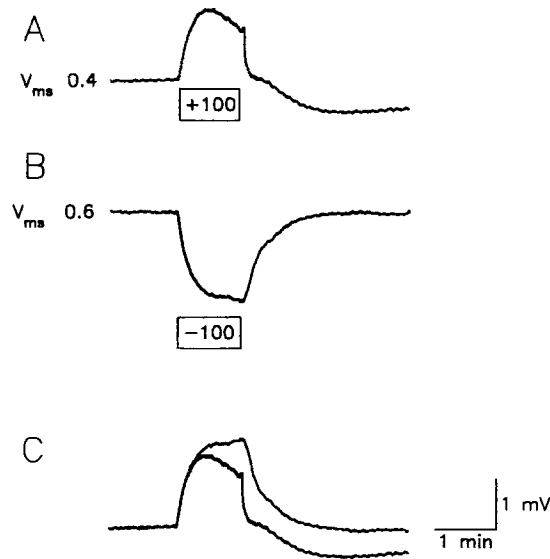
A

V_{ms} 0.4 ────────── +100

B

V_{ms} 0.6 ────────── −100

C

1 mV

1 min

FIGURE 3. Comparison of the effects of addition of 100 mM sucrose (A) and removal of 100 mM sucrose (B) on the transepithelial voltage. In C, trace B was inverted and superimposed with trace A. Note that the absolute values of the initial rates of change of V_{ms} are identical, but that later on V_{ms} decreases in hyperosmotic solution and increases in hypoosmotic solution.

no significant contribution of alterations in the electrical parameters of the cell membranes (zero-current voltage and resistance) to the V_{ms} change.

To assess the possible contribution of events at the cell membranes on the observed changes in transepithelial voltages, we carried out intracellular microelectrode experiments such as that illustrated in Fig. 4. Measurements in several tissues are summarized in Table IV. Addition of sucrose to the apical bathing solution caused a mucosa-positive change in transepithelial voltage, a significant, although small, depolarization of the basolateral membrane, no significant change in apical membrane potential (after 1 min), a decrease in the fractional resistance of the apical membrane ($fR_a = R_a/[R_a + R_{bl}]$), and an increase in transepithelial resistance (R_t). Upon return to control solution, there was a slow and transient hyperpolarization of both cell membranes, with monotonic restoration of R_t and fR_a. Exposure to a hypoosmotic solution (sucrose removal) caused a biphasic change in cell membrane voltages (depolarization followed by hyperpolarization), an increase in fR_a, and a decrease in R_t. The resistance changes are opposite to those elicited by the

TABLE III

Comparison between the Effects of Increasing and Decreasing Mucosal Solution Osmolality on Transepithelial Voltage

Osmolality	Transepithelial voltage			
	Control	Peak	1 min	Control
mosmol/kg		mV		
+100	−0.2 ± 0.2	1.9 ± 0.5*	1.7 ± 0.4*	−0.3 ± 0.2
−100	0.1 ± 0.3	−1.7 ± 0.3*	−2.3 ± 0.3*	−0.1 ± 0.3

Data are means ± SEM, n = 6 paired experiments. Post-control values were measured 5 min after returning to the standard Ringer's solution.
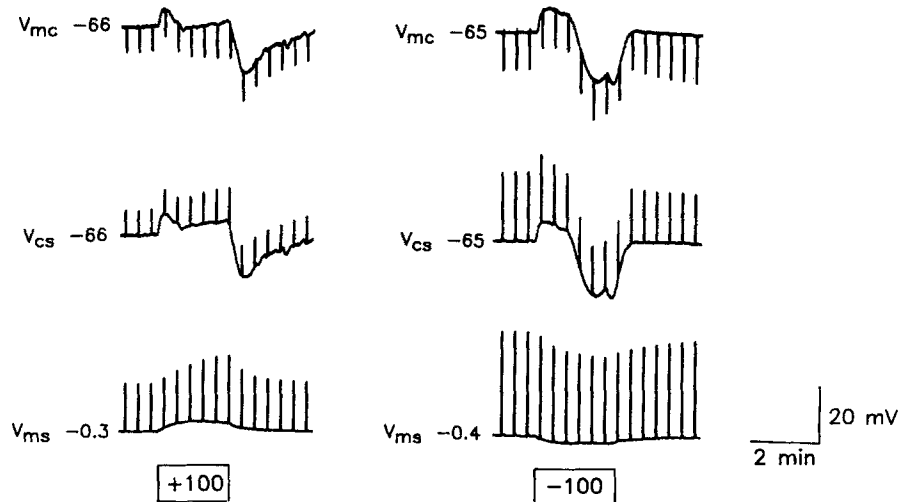*Significantly different from control (P < 0.05).

FIGURE 4. Effects of addition of 100 mM sucrose (*left*) or removal of 100 mM sucrose (*right*) on cell membrane and transepithelial electrical parameters. V_{mc}, apical membrane voltage; V_{cs}, basolateral membrane voltage; V_{ms}, transepithelial voltage. Polarity conventions: $V_{mc} = V_c - V_m$; $V_{cs} = V_c - V_s$; $V_{ms} = V_m - V_s$. The starting voltages are indicated for each record. Upward voltage deflections denote positive voltage changes. Periods of changes in osmolality are indicated by the bars. The brief voltage deflections were produced by transepithelial constant current pulses of 50 μA · cm^{-2} and 1-s duration at 20-s intervals; fR_a and R_t were calculated from these data after correction for series resistances. The different control values of fR_a and R_t in the right-hand panels are due to the lower starting [NaCl] (see Table IV and text).

TABLE IV

Effects of Changes in Apical Solution Osmolality on Transepithelial and Cell–Membrane Electrical Parameters

Osmolality	V_{ms}	V_{mc}	V_{cs}	fR_a	R_t
mosmol/kg	*mV*	*mV*	*mV*		Ω cm^2
Control	−0.3 ± 0.2	−66 ± 3	−66 ± 3	0.85 ± 0.03	187 ± 14
+100, 1 min	2.7 ± 0.3*	−67 ± 4	−64 ± 4	0.63 ± 0.01*	363 ± 33*
+100, 2 min	3.0 ± 0.2*	−68 ± 5	−66 ± 5	0.61 ± 0.01*	386 ± 41*
Control	−0.1 ± 0.3	−67 ± 4	−67 ± 4	0.79 ± 0.05	192 ± 13
Control	−0.6 ± 0.4	−61 ± 3	−61 ± 3	0.84 ± 0.04	197 ± 18
+200, 1 min	4.6 ± 0.8*	−59 ± 4	−54 ± 3*	0.48 ± 0.02*	493 ± 44*
+200, 2 min	3.2 ± 0.5*	−58 ± 3	−55 ± 3*	0.38 ± 0.04*	575 ± 34*
Control	−0.4 ± 0.4	−59 ± 3	−59 ± 3	0.71 ± 0.04	229 ± 22
Control	−0.9 ± 0.9	−70 ± 4	−71 ± 4	0.62 ± 0.08	430 ± 27
−100, 1 min	−5.8 ± 1.6*	−74 ± 5	−80 ± 3*	0.80 ± 0.04*	259 ± 24*
−100, 2 min	−5.8 ± 1.7*	−77 ± 2	−83 ± 2*	0.85 ± 0.06*	221 ± 24*
Control	−1.1 ± 0.7	−70 ± 4	−71 ± 4	0.76 ± 0.06	410 ± 35

Data are means ± SEM of $n = 7$ experiments. In each group of experiments the four lines denote control values, experimental values at 1 and 2 min, and control values at ~3 min after returning to control bathing solution. + indicates an increase in osmolality by addition of sucrose and − indicates a decrease in osmolality by removal of sucrose.

*Significantly different from control ($P < 0.05$).

hyperosmotic bathing solution. In experiments with the same bathing solution as the NaCl-Ringer's used in the present studies, the steady-state electrical resistance of the two cell membranes in series is ~45-fold that of the paracellular pathway (Stoddard and Reuss, 1988a). Therefore, if the changes in V_{ms} elicited by anisosmotic solutions were caused by events at the cell membranes, the concomitant changes in cell membrane voltages would be ~45-fold greater. The results summarized in Table IV clearly indicate that although some changes in cell membrane voltages do occur, their magnitudes are small. In conclusion, the intracellular-microelectrode data indicate that the V_{ms} changes produced by exposure to anisosmotic apical bathing solutions are of paracellular origin. This issue is addressed in detail in the Discussion.

Time Course of the Changes in Transepithelial Voltage

A consistent observation in these studies was that the early changes in transepithelial voltage upon addition or removal of sucrose from the apical bathing solution appear slow relative to the changes in sucrose concentration near the epithelial surface. To quantitate this phenomenon we carried out paired experiments in which the time course of the apparent streaming potential (sucrose addition) was compared with that of a bi-ionic paracellular diffusion potential produced by replacing part of the NaCl with TBA$^+$ chloride in the apical bathing solution. The rationale for the choice of TBA$^+$ as an impermeant Na$^+$ substitute is that the diffusion coefficients of sucrose and TBACl are very similar (Cotton and Reuss, 1989). Therefore, TBA$^+$ can be used as a sucrose "tracer," i.e., the TBA$^+$ concentration near the cell surface, monitored with a microelectrode, denotes the time course of the change in sucrose concentration. The main point is that in the bi-ionic potential experiment (partial replacement of Na$^+$ with TBA$^+$) and in the osmotic experiment (addition of sucrose with TBA$^+$ as a tracer) the time courses of the relevant concentration changes at the cell surface should be similar. It is likely that the time course of the change in [TBA$^+$] at the cell surface is not exactly the same in the two experimental conditions: when TBA$^+$ replaces Na$^+$ (bi-ionic potential), a liquid junction potential is established at the interface between the NaCl/TBACl solution and the NaCl solution near the cell surface. Inasmuch as Na$^+$ has a higher mobility than TBA$^+$, the potential tends to speed up TBA$^+$ diffusion to the cell surface. However, both solutions contain ~98 mM Cl$^-$; since the Cl$^-$ mobility is higher than those of Na$^+$ and TBA$^+$, the liquid junction potential is small, and hence TBA$^+$ arrival to the cell surface deviates only slightly from the expectations for simple diffusion.

The result of the experiment is illustrated in Fig. 5. The transepithelial voltage changes in response to changes in sucrose concentration (apparent streaming potentials) were much slower that those elicited by the Na$^+$/TBA$^+$ substitution (bi-ionic diffusion potential). In Table V we summarize results from experiments in several tissues. If the effects of the Na$^+$/TBA$^+$ substitution and the addition of sucrose are exerted at the same site in the junctions, the slow voltage changes in the latter condition are inconsistent with a "true" streaming potential, as will be shown in the accompanying paper (Reuss et al., 1992).

A second observation, illustrated in Figs. 1 and 3, is that during exposure to hyperosmotic solutions V_{ms} decreases after reaching a maximum value, whereas in hypoosmotic solutions the change in V_{ms} increases with time. These observations indicate that the apparent ion selectivity and/or the ion concentration gradients
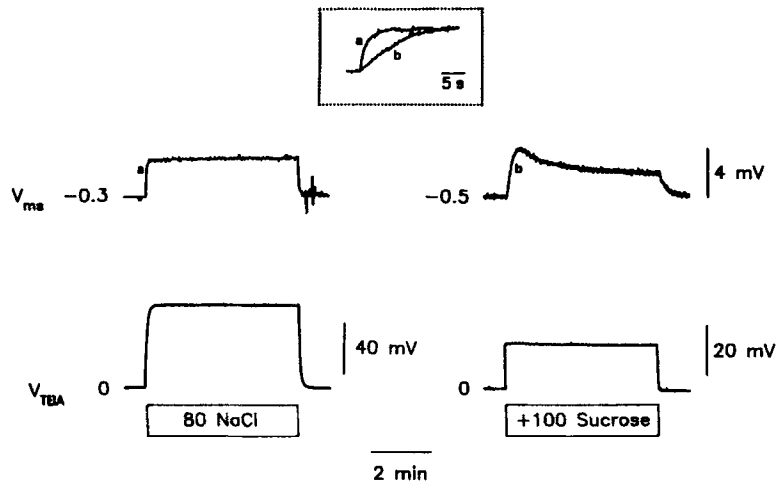
FIGURE 5. Time courses of V_{ms} and V_{TBA} upon replacement of 20 mM NaCl with TBACl (bi-ionic potential; *left*) or addition of 100 mM sucrose to the apical bathing solution (apparent streaming potential; *right*). The inset on top shows the early time courses of V_{ms} on an expanded time axis. Note that the change in V_{ms} is much faster in the bi-ionic than in the apparent streaming potential.

across the paracellular pathway change during the period of exposure to the anisosmotic solution, decreasing with hyperosmotic challenge and increasing with hypoosmotic challenge. Three mechanisms must be considered to interpret these changes: (a) The water flows elicited by the transepithelial osmotic gradients cause changes in the width of the lateral intercellular spaces (narrowing with apical hyperosmotic solution and widening with apical hypoosmotic solution). (b) The water flows from or into the basolateral surface of the cells cause changes in ionic strength of the solution in the lateral spaces, which via changes in surface potential of the ion-selective pathway could alter its selectivity. (c) The changes in ion concentrations change the conductivity of the solution in the lateral intercellular spaces. While (a) and (b) are changes in the right direction to account for the experimental observations, the changes in fluid conductivity are opposite; i.e., with hyperosmotic apical

TABLE V

Comparison of the Time Courses of Apparent Streaming Potentials and Bi-ionic Potentials

	Voltage change	Half-time on	Half-time off
	mV	*s*	*s*
Streaming			
50 mosmol/kg	2.3 ± 0.3*	9.0 ± 0.5*	9.5 ± 0.4*
100 mosmol/kg	3.8 ± 0.6	7.5 ± 0.8*	8.8 ± 0.6*
200 mosmol/kg	6.7 ± 0.9*	6.2 ± 0.4*	8.4 ± 0.9*
Bi-ionic	3.2 ± 0.2	2.3 ± 0.5	1.6 ± 0.4

Data are means ± SEM, $n = 6$ paired experiments.
*Significantly different from analogous value in the bi-ionic potential experiment ($P < 0.05$).

solution the spaces will narrow down (tending to increase R_t), but the fluid conductivity will increase (tending to decrease R_t). Hence, the change in R_t is the net effect of these two opposite mechanisms.

The role of changes in R_t on the late V_{ms} changes was addressed experimentally by measuring the transepithelial resistance changes during osmotic challenges. Data before and 1 and 2 min after exposure to anisosmotic solutions are presented in Table IV, and an experiment showing a more detailed time course is shown in Fig. 6. The observed changes in transepithelial resistance are consistent with a dominant effect of a reduction in lateral intercellular space width in tissues exposed to hyperosmotic solution and with widening of the spaces during exposure to hypoosmotic solutions.

To assess the role of ionic strength on ion selectivity, we carried out experiments in which the ionic strength and the osmolality of the basolateral bathing solution were increased by addition of 25 or 50 mM NaCl. The change in V_{ms} elicited by partial
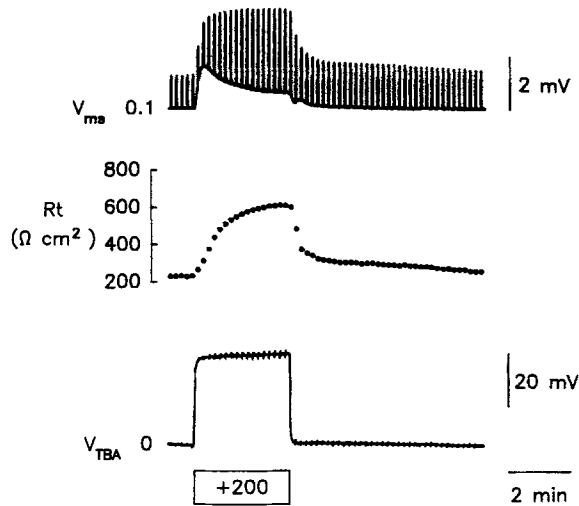

FIGURE 6. Changes in transepithelial resistance during sucrose addition (200 mM) to the apical bathing solution. (*Top*) V_{ms}; transepithelial current pulses: 50 μA · cm^{-2}, 1-s duration, 10-s interval. (*Middle*) R_t, calculated for every pulse from the voltage deflections in the V_{ms} trace after correction for series resistance. (*Bottom*) V_{TBA}. Note that the decline of V_{ms} and the increase in R_t have similar time courses, and that both are slow relative to the change in V_{TBA}.

replacement of Na$^+$ with TBA$^+$ was measured during steady-state basolateral exposure to control Ringer's solution and to solutions with elevated [NaCl]. The magnitude of the bi-ionic potential was the same in all conditions, indicating no significant differences in junctional selectivity. In four experiments, the changes in V_{ms} were 3.1 ± 0.1 mV in control Ringer's, 3.3 ± 0.1 mV in Ringer's + 25 mM NaCl, 3.4 ± 0.2 mV in Ringer's + 50 mM NaCl, and 3.3 ± 0.1 mV upon returning to control Ringer's solution.

DISCUSSION

General Characteristics of Apparent Streaming Potentials in Necturus Gallbladder Epithelium

Addition of the impermeant nonelectrolyte sucrose to the NaCl Ringer's solution bathing the apical surface of *Necturus* gallbladder epithelium produces lumen-

positive changes in transepithelial voltage with complex time courses (see below). The maximum values of the voltage changes are greater with higher sucrose concentrations. Changes in transepithelial voltage upon osmotic challenges similar to those described here have been reported in several leaky epithelia (Pidot and Diamond, 1964; Diamond and Harrison, 1966; Frömter and Gessner, 1974; De Mello et al., 1976; Corman, 1985; Tripathi and Boulpaep, 1988). When the tissues are initially exposed to salt solutions of physiologic composition, the polarity of the apparent streaming potentials is lumen positive in rabbit gallbladder (Pidot and Diamond, 1964; Diamond and Harrison, 1966), *Necturus* gallbladder (Reuss and Finn, 1977), and rat kidney proximal tubule (Frömter and Gessner, 1974; see also De Mello et al., 1976). In rabbit proximal convoluted tubule, the apparent streaming potential can be either lumen positive or lumen negative when the peritubular solution is rendered hyperosmotic by addition of raffinose, depending on whether the tubules were dissected from mid-cortical or juxtamedullary regions (Corman, 1985). In *Ambystoma* proximal tubule, sucrose addition to the luminal solution produced a lumen-negative voltage change (Tripathi and Boulpaep, 1988). In all cases, the polarity of the apparent streaming potential observed in preparations bathed with symmetric NaCl-based solutions was consistent with the overall ionic selectivity of the epithelium, assessed by transepithelial dilution potentials, i.e., by unilateral reductions in [NaCl] under isosmotic conditions (NaCl replaced with sucrose or other nonelectrolytes). Therefore, these observations correspond to apparent streaming potentials, which in principle could be explained by coupling between water and ion fluxes in an ion-selective pathway (true streaming potential) or by a salt concentration gradient produced across the epithelium because of the water flow elicited by the osmotic gradient. Regardless of which of these mechanisms is responsible for the observed voltage changes, it is likely that the site of production of the apparent streaming potential is paracellular, because in gallbladder epithelium and in renal proximal tubules the paracellular ion conductance is much higher than the ion conductances of the cell membranes (Frömter, 1972; Reuss and Finn, 1975a, b; Guggino et al., 1982; Stoddard and Reuss, 1988a). However, definitive conclusions on the site of origin of the apparent streaming potential require measurements of cell membrane voltages and conductances. Such measurements have only been reported by Tripathi and Boulpaep (1988) for *Ambystoma* proximal tubule, and are lacking for gallbladder epithelium. Tripathi and Boulpaep (1988) ruled out a significant contribution of cell membrane events to their observations.

Studies of paracellular ion selectivity in *Necturus* gallbladder epithelium have demonstrated that the junctional complexes are cation selective, with the sequence $P_K > P_{Na} > P_{Li}$ (Reuss and Finn, 1975a; Van Os and Slegers, 1975); from transepithelial dilution potentials (data not shown) P_{Na}/P_{Cl} is ~ 5. Complete replacement of Na^+ with TMA^+ or N-methyl-D-glucammonium ($NMDG^+$) increases considerably the transepithelial resistance (Reuss and Finn, 1975a), but not to levels comparable to those of the cell membranes in series, suggesting that the paracellular Cl^- permeability, although small, is significant. Confirmation of this view was obtained in the experiments in which Na^+ was replaced on both sides with TMA^+. Under these conditions, the sign of the apparent streaming potential was reversed (Fig. 2, Table II), indicating that at the relevant permeation pathway $P_{Cl} > P_{TMA}$. As expected from

the high value of P_{Na}/P_{Cl}, replacing Cl⁻ with cyclamate had no significant effect on the voltage change elicited by addition of sucrose to the apical solution. When the main salt in both solutions was TMA-cyclamate, sucrose addition caused no significant change in transepithelial voltage, suggesting that TMA⁺ and cyclamate have similar electrodiffusive permeabilities, and from the sign reversal of the potential change in TMACl, obviously much smaller than P_{Na} and P_{Cl}. In summary, the results presented indicate that the apparent streaming potentials elicited across *Necturus* gallbladder epithelium under a variety of ion substitutions have the characteristics expected for a paracellular origin. Further evidence for this conclusion is discussed in the next section.

Paracellular Origin of Apparent Streaming Potentials

Direct demonstration of the paracellular origin of a transepithelial voltage change requires measurements of cell membrane electrical parameters and circuit analysis to
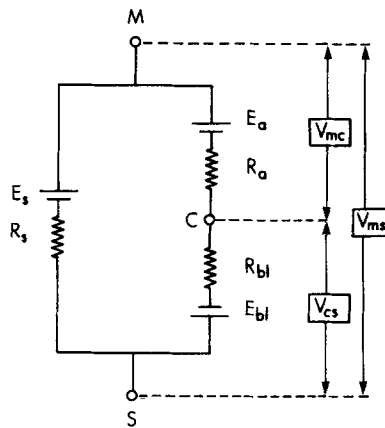

FIGURE 7. Steady-state, passive equivalent electrical circuit for *Necturus* gallbladder epithelium. M, C, and S represent mucosal solution, cell, and serosal solution, respectively. Cell membranes and paracellular pathway are depicted as Thévenin equivalents (equivalent electromotive force, E, in parallel with resistance, R). The subscripts a, bl, and s denote apical membrane, basolateral membrane, and paracellular (shunt) pathway, respectively. V_{ms}, V_{mc}, and V_{cs} are the transepithelial, apical membrane, and basolateral membrane voltages (polarity conventions: $V_{ms} = V_m - V_s$; $V_{mc} = V_c - V_m$; $V_{cs} = V_c - V_s$).

establish the contributions of cell membranes and paracellular pathway to the change in V_{ms}. This analysis was based on the equivalent electrical circuit depicted in Fig. 7 (see Reuss and Finn, 1975a). The value of V_{ms} in any condition is given by

$$V_{ms} = \frac{(E_{bl} - E_a) R_s + E_s (R_a + R_{bl})}{R_a + R_{bl} + R_s}$$

(1)

where E and R denote zero-current voltages and resistances, respectively, and the subscripts a, bl, and s refer to the apical membrane, the basolateral membrane, and the paracellular pathway, respectively (see Reuss and Finn, 1975a, b). Polarity conventions are as follows: V_{ms} and E_s are referred to the basolateral solution; cell membrane voltages and zero-current voltages are referred to the adjacent bathing solutions.

In principle, alterations in any of the above parameters can change V_{ms}. An assessment of relative contributions of cellular and paracellular events can be

obtained by considering the analogous equations for the cell membrane voltages:

$$V_{mc} = \frac{E_a \, (R_{bl} + R_s) + (E_{bl} - E_s) \, R_a}{R_a + R_{bl} + R_s} \tag{2}$$

$$V_{cs} = \frac{E_{bl} \, (R_a + R_s) + (E_a + E_s) \, R_{bl}}{R_a + R_{bl} + R_s} \tag{3}$$

where V_{mc} and V_{cs} are the apical and basolateral membrane voltages, respectively (polarity conventions as defined above). The essential point of the analysis can be made by considering the effects of a change in cell membrane zero-current voltage (for instance E_a) on V_{ms} and V_{mc}, all other parameters remaining constant:

$$\Delta V_{ms} = \frac{-\Delta E_a R_s}{R_a + R_{bl} + R_s} \tag{4}$$

$$\Delta V_{mc} = \frac{\Delta E_a \, (R_{bl} + R_s)}{R_a + R_{bl} + R_s} \tag{5}$$

The ratio of the changes ($\Delta V_{ms}/\Delta V_{mc}$) is given by $-R_s/(R_{bl} + R_s)$, which under control conditions is ~ 0.17 (Stoddard and Reuss, 1988a). In other words, a change in E_a sufficient to change V_{ms} by 3 mV (100 mM sucrose, Table IV) should have hyperpolarized the apical membrane by 17.6 mV. In contrast, V_{mc} did not change significantly. The case for a primary change in E_{bl} is even stronger, because the value of R_s/R_a is 0.02 (Stoddard and Reuss, 1988a). Although significant changes in V_{cs} were observed with addition of 200 mM sucrose and with removal of 100 mM sucrose, these changes were too small to account for a significant fraction of the transepithelial voltage change. Hence, we conclude that the apparent streaming potential changes observed cannot be explained by primary changes in zero-current membrane voltages.

A second possibility is that the change in V_{ms} is the consequence of the concomitant change in R_s, which is approximated by the change in R_t depicted in Table IV. This change is unlikely to explain the initial portion of the apparent streaming potential, for the following reasons: (a) E_a and E_{bl} have similar values under control conditions (Stoddard and Reuss, 1988a, 1989), and therefore the product $(E_{bl} - E_a)R_s$ is near zero regardless of the value of R_s. (b) The change in R_s is slower than the change in V_{ms}. (c) When R_s increases during the hyperosmotic challenge, V_{ms} is reduced from its maximum value to a voltage closer to the control one (Fig. 6). This effect is opposite in direction to the one expected if the increase in R_s contributes to the initial phase of the V_{ms} change. A similar argument can be made for the possible role of R_s on the V_{ms} changes upon hypoosmotic challenge. In conclusion, changes in R_s do not play a significant role in the early phases of the apparent streaming potentials. Nevertheless, they appear to contribute to the late changes in V_{ms}. This is discussed in detail below.

A third possibility is that the changes in V_{ms} elicited by anisosmotic solutions are due to primary changes in one or both cell membrane resistances. The fractional resistance of the apical membrane changes significantly during exposure to either hyper- or hypoosmotic apical bathing solutions (Table IV, Fig. 4), indicating alteration of R_a, R_{bl}, or both. A contribution of cell membrane resistance changes to

the change in transepithelial voltage elicited by the hyperosmotic solution would require a very large fall in both R_a and R_{bl} (see Eq. 1). Definitive elimination of this hypothesis is possible only by direct assessment of cell membrane resistances, which in this preparation requires cable analysis. This was not done in the present study, but during steady-state exposure to a hyperosmotic apical bathing solution the steady-state change in the resistances of the two cell membranes, in series, was from 8,100 to 5,400 $\Omega \cdot cm^2$ (Reuss and Finn, 1977), a change insufficient to explain the transepithelial voltage change. As in the case of the effects of alterations in R_s, discussed above, changes in R_a and R_{bl} could contribute to the slow transepithelial voltage transients observed after the faster initial changes.

Although contributions of changes in cell membrane conductances and zero-current voltages to the transepithelial streaming potentials can be ruled out based on the above arguments, clearly there are significant changes in cell membrane voltages and in the fractional resistance of the apical membrane, as shown in Table IV. It is possible that the changes in fractional resistance are in part due to changes in lateral intercellular space width (narrowing in hyperosmotic solution and widening in hypoosmotic solution), which can have large effects on the distributed equivalent circuit of lateral membrane and lateral space (Boulpaep and Sackin, 1980). However, in recent intracellular cable analysis experiments in which large transepithelial resistance changes were elicited by transepithelial current pulses, we observed no changes in the resistance of the two cell membranes in parallel (Stoddard and Reuss, 1988b). Alternatively, the changes in cell membrane properties could correspond to ion conductance changes in response to the changes in cell volume expected to result from the alterations of apical bathing solution osmolality. Experimental results to be published separately suggest that cell shrinkage decreases the basolateral membrane conductance, whereas cell swelling increases basolateral membrane conductance. The conductance changes appear to involve mainly g_K, but also to some extent g_{Cl}. The changes in V_{cs} and fR_a observed in these studies agree with this interpretation.

In conclusion, our studies indicate that the site of origin of the apparent streaming potentials elicited by changes in apical solution osmolality in *Necturus* gallbladder is the paracellular pathway. This conclusion agrees with that reached by Tripathi and Boulpaep (1988) in their studies in *Ambystoma* proximal tubule. These authors speculated further that the precise site of origin was the lateral space and not the tight junction. This issue will be discussed further in the accompanying paper (Reuss et al., 1992). Here, we will conclude by stating that every observation presented is consistent with a junctional site of origin of the apparent streaming potential, and at least one observation argues against the lateral intercellular space origin. The observation is that the directions of the voltage transients after the peak changes in V_{ms} were opposite to those expected from the changes in R_t. In other words, with hyperosmotic solutions on the apical side R_t increased while V_{ms} declined, and with hypoosmotic solutions decreases in R_t occurred concomitantly with increases in the value of V_{ms}. Tripathi and Boulpaep (1988) suggested that the lateral space is the site of origin of the streaming potential. If the changes of R_t elicited by osmotic challenges reflect changes in lateral space width, as widely accepted (Frömter, 1972; Spring and Hope, 1978, 1979; Stoddard and Reuss, 1988b), then the transepithelial

voltage changes should increase as the spaces collapse because the fractional resistance of the junctions vis-a-vis the spaces would decrease.

Time Course of Apparent Streaming Potentials

The time course of the apparent streaming potentials is complex. A first observation is that the V_{ms} changes at both the onset and termination of the osmotic challenge are too slow relative to the changes in sucrose concentration near the cell surface. This is the case for both hyper- and hypoosmotic challenges. The comparison between sucrose-induced apparent streaming potentials and TBA^+/Na^+ bi-ionic potentials (Fig. 5) indicates that the former is much slower than the latter. This occurs although the diffusion coefficients of sucrose and TBACl are very close, and therefore the time courses of the changes in their concentrations at the cell surface should be similar. If bi-ionic and streaming potentials originate at the same site, then a "true" streaming potential and a bi-ionic potential should have the same time course. In contrast, the half-times for development of apparent streaming potentials were three- to six-fold those measured for paired bi-bionic potentials. This observation cannot be reconciled with the hypothesis of a true streaming potential unless the streaming potential and the bi-ionic potential originated at separate sites. Data presented in the accompanying paper rule out the latter possibility and support the conclusion that the apparent streaming potentials in *Necturus* gallbladder epithelium are in fact pseudo-streaming potentials.

A last issue to discuss pertains to the transient voltage changes during exposure to either hyper- or hypoosmotic solutions. The most likely mechanism is the change in the paracellular electrical resistance, which is the result of two factors operating in opposite directions, namely, a decrease in cross-sectional area of the zonula adherens and/or the lateral intercellular space, and the increase in fluid conductivity in the space. The experimental observation of an increase in R_t indicates that the first mechanism dominates. Cable analysis experiments during long-term transepithelial current clamps yield large changes in R_t attributable to transport-number effects (Barry and Hope, 1969a, b; see also Stoddard and Reuss, 1988b). However, the change in R_t is not accompanied by changes in apparent basolateral membrane resistance (R_{bl}) (Stoddard and Reuss, 1988b). With apical-to-basolateral current flow (equivalent to apical hyperosmotic solution) a homogeneous narrowing of the lateral spaces would be expected to elevate R_{bl}, which is the equivalent resistor of a distributed circuit (basal membrane and lateral membrane in series with the intercellular spaces). The lack of change of R_{bl} suggests that the narrowing of the spaces may be restricted to their apical end (Stoddard and Reuss, 1988b). In any event, since the space is a resistor in series with the junction, the net effect of an increase in its resistance is to reduce the change in V_{ms}, although E_s could remain unchanged. Inasmuch as the paracellular ion selectivity of the epithelium depends on fixed charges (Wright and Diamond, 1968; Diamond and Wright, 1969; Wright, Barry, and Diamond, 1971), we investigated the possible role of changes in ionic strength of the lateral space fluid in the V_{ms} transients. An increase in ionic strength could screen fixed negative charges, reducing P_{Na}/P_{Cl} and therefore the value of the streaming potential. This possibility was ruled out by measurements of bi-ionic (Na^+/TBA^+)

potentials under control conditions and after raising the [NaCl] in the basolateral bathing medium.

In summary, apparent streaming potentials (probably pseudo-streaming potentials) can be elicited across *Necturus* gallbladder epithelium by rapid exposure to anisosmotic apical bathing solutions. A quantitative analysis of these transepithelial voltage changes is presented in the accompanying paper (Reuss et al., 1992).

REFERENCES

Altenberg, G., J. Copello, C. Cotton, K. Dawson, Y. Segal, F. Wehner, and L. Reuss. 1990. Electrophysiological methods for studying ion and water transport in *Necturus* gallbladder epithelium. *Methods in Enzymology.* 192:650–683.

Barry, P. H. 1989. Ionic permeation mechanisms in epithelia: biionic potentials, dilution potentials, conductances, and streaming potentials. *Methods in Enzymology.* 171:687–714.

Barry, P. H., and J. M. Diamond. 1984. Effects of unstirred layers on membrane phenomena. *Physiological Reviews.* 64:763–873.

Barry, P. H., and A. B. Hope. 1969a. Electroosmosis in membranes: effects of unstirred layers and transport numbers. I. Theory. *Biophysical Journal.* 9:700–728.

Barry, P. H., and A. B. Hope. 1969b. Electroosmosis in membranes: effects of unstirred layers and transport numbers. II. Experimental. *Biophysical Journal.* 9:729–757.

Berry, C. A. 1983. Water permeability and pathways in the proximal tubule. *American Journal of Physiology.* 245:F279–F294.

Boulpaep, E. L., and H. Sackin. 1980. Electrical analysis of intraepithelial barriers. *Current Topics in Membranes and Transport.* 13:169–197.

Corman, B. 1985. Streaming potentials and diffusion potentials across rabbit proximal convoluted tubule. *Pflügers Archiv.* 403:156–163.

Cotton, C. U., and L. Reuss. 1989. Measurement of the effective thickness of the mucosal unstirred layer in *Necturus* gallbladder. *Journal of General Physiology.* 93:631–647.

Cotton, C. U., A. M. Weinstein, and L. Reuss. 1989. Osmotic water permeability of *Necturus* gallbladder. *Journal of General Physiology.* 93:649–679.

De Mello, G. B., A. G. Lopes, and G. Malnic. 1976. Conductances, diffusion and streaming potentials in the rat proximal tubule. *Journal of Physiology.* 260:553–569.

Diamond, J. M. 1979. Osmotic water flow in leaky epithelia. *Journal of Membrane Biology.* 51:195–216.

Diamond, J. M., and S. C. Harrison. 1966. The effect of membrane fixed charges on diffusion potentials and streaming potentials. *Journal of Physiology.* 183:37–57.

Diamond, J. M., and E. M. Wright. 1969. Biological membranes: the physical basis of ion and nonelectrolyte selectivity. *Annual Review of Physiology.* 31:581–646.

Finkelstein, A. 1987. Water movement through lipid bilayers, pores and plasma membranes. *In* Distinguished Lecture Series of the Society of General Physiologists. Vol. 4. John Wiley & Sons, Inc., New York. 58, 144.

Frömter, E. 1972. The route of passive ion movement through the epithelium of *Necturus* gallbladder. *Journal of Membrane Biology.* 8:259–301.

Frömter, E., and K. Gessner. 1974. Active transport potentials, membrane diffusion potentials and streaming potentials across rat kidney proximal tubule. *Pflügers Archiv.* 361:85–98.

Guggino, W. B., E. E. Windhager, E. L. Boulpaep, and G. Giebisch. 1982. Cellular and paracellular resistances of the *Necturus* proximal tubule. *Journal of Membrane Biology.* 67:143–154.

Hill, A. E. 1975a. Solute-solvent coupling in epithelia: an electro-osmotic theory of fluid transfer. *Proceedings of the Royal Society of London B.* 190:115–134.

Hill, A. E. 1975b. Solute-solvent coupling in epithelia: contribution of the junctional pathway to fluid production. *Proceedings of the Royal Society of London B.* 191:537–547.

Hill, A. E. 1980. Salt-water coupling in leaky epithelia. *Journal of Membrane Biology.* 56:177–182.

Hill, A. E., and B. S. Hill. 1978a. Sucrose fluxes and functional water flow across *Necturus* gallbladder epithelium. *Proceedings of the Royal Society of London B.* 200:163–174.

Hill, B. S., and A. E. Hill. 1978b. Fluid transfer by *Necturus* gallbladder epithelium as a function of osmolarity. *Proceedings of the Royal Society of London B.* 200:151–162.

House, C. R. 1974. Water Transport in Cells and Tissues. Edward Arnold Ltd., London. 97–102, 141–144.

Meyer, M. M., and A. S. Verkman. 1987. Evidence for water channels in renal proximal tubule cell membranes. *Journal of Membrane Biology.* 96:107–119.

Mollgard, K., and J. Rostgaard. 1978. Morphological aspects of some sodium transporting epithelia suggesting a transcellular pathway via elements of endoplasmic reticulum. *Journal of Membrane Biology.* 40:71–89.

Persson, B.-E., and K. R. Spring. 1982. Gallbladder epithelial cell hydraulic water permeability and volume regulation. *Journal of General Physiology.* 79:481–505.

Pidot, A. L., and J. M. Diamond. 1964. Streaming potentials in a biological membrane. *Nature.* 201:701–702.

Reuss, L. 1989. Ion transport across gallbladder epithelium. *Physiological Reviews.* 69:503–545.

Reuss, L., and C. U. Cotton. 1988. Isosmotic fluid transport across epithelia. *Contemporary Nephrology.* 4:1–37.

Reuss, L., and A. L. Finn. 1975a. Electrical properties of the cellular transepithelial pathway in *Necturus* gallbladder. I. Circuit analysis and steady-state effects of mucosal solution ionic substitutions. *Journal of Membrane Biology.* 26:115–139.

Reuss, L., and A. L. Finn. 1975b. Electrical properties of the cellular transepithelial pathway in *Necturus* gallbladder. II. Ionic permeability of the apical cell membrane. *Journal of Membrane Biology.* 26:141–161.

Reuss, L., and A. L. Finn. 1977. Effects of luminal hyperosmolality on electrical pathways of *Necturus* gallbladder. *American Journal of Physiology.* 232:C99–C108.

Reuss, L., B. Simon, and C. U. Cotton. 1992. Pseudo-streaming potentials in *Necturus* gallbladder epithelium. II. The mechanism is a junctional diffusion potential. *Journal of General Physiology.* 92:297–316.

Sackin, H., and E. Boulpaep. 1975. Models for coupling of salt and water transport. Proximal tubular reabsorption in *Necturus* kidney. *Journal of General Physiology.* 66:671–733.

Schafer, J. A. 1990. Transepithelial osmolality differences, hydraulic conductivities, and volume absorption in the proximal tubule. *Annual Review of Physiology.* 52:709–726.

Spring, K. R. 1991. Mechanism of fluid transport by epithelia. *In* Handbook of Physiology. Section 6. The Gastrointestinal System. Vol. IV. Intestinal Absorption and Secretion. S. G. Schultz, M. Field, and R. A. Frizzel, editors. Oxford University Press, New York. 195–208.

Spring, K. R., and A. Hope. 1978. Size and shape of the lateral intercellular spaces in a living epithelium. *Science.* 200:54–58.

Spring, K. R., and A. Hope. 1979. Fluid transport and the dimensions of cells and interspaces of living *Necturus* gallbladder. *Journal of General Physiology*. 73:287–305.

Stoddard, J., and L. Reuss. 1988a. Dependence of cell membrane conductances on bathing solution HCO_3^-/CO_2 in *Necturus* gallbladder. *Journal of Membrane Biology*. 102:163–174.

Stoddard, J. S., and L. Reuss. 1988b. Voltage- and time-dependence of apical membrane conductance during current clamp in *Necturus* gallbladder epithelium. *Journal of Membrane Biology*. 103:191–204.

Stoddard, J. S., and L. Reuss. 1989. pH effects on basolateral membrane ion conductances in gallbladder epithelium. *American Journal of Physiology*. 256:C1184–C1195.

Tripathi, S., and E. L. Boulpaep. 1988. Cell membrane water permeabilities and streaming currents in *Ambystoma* proximal tubule. *American Journal of Physiology*. 254:F188–F203.

Tripathi, S., and E. L. Boulpaep. 1989. Mechanisms of water transport by epithelial cells. *Quarterly Journal of Experimental Physiology*. 74:385–417.

Van Os, C. H., and J. F. G. Slegers. 1975. The electrical potential profile of gallbladder epithelium. *Journal of Membrane Biology*. 24:341–363.

Verkman, A. S. 1989. Mechanisms and regulation of water permeability in renal epithelia. *American Journal of Physiology*. 257:C837–C850.

Weinman, S. A., and L. Reuss. 1984. Na^+-H^+ exchange and Na^+ entry across the apical membrane of *Necturus* gallbladder. *Journal of General Physiology*. 83:57–74.

Weinstein, A. M., J. L. Stephenson, and K. R. Spring. 1981. The coupled transport of water. *In* Membrane Transport. S. L. Bonting, and J. J. H. H. M. de Pont, editors. Elsevier/North Holland Biomedical Press, Amsterdam. 311–351.

Whittembury, G., and P. Carpi-Medina. 1988. Renal absorption of water: are there pores in proximal tubule cells? *News in Physiological Sciences*. 3:61–65.

Whittembury, G., C. V. de Martínez, A. Paz-Aliaga, and H. Linares. 1981. Paracellular water flow in leaky epithelia: evidence from solvent drag of extracellular solutes. *In* Water Transport Across Epithelia: Barriers, Gradients and Mechanisms. H. H. Ussing, N. A. Bindslev, N. A. Lassen, and O. Sten-Knudsen, editors. Munksgaard, Copenhagen. 17–35.

Whittembury, G., and L. Reuss. 1991. Mechanisms of coupling of solute and solvent transport in epithelia. *In* The Kidney: Physiology and Pathophysiology. D. W. Seldin and G. Giebisch, editors. Raven Press, New York. 316–360.

Wright, E. M., P. H. Barry, and J. M. Diamond. 1971. The mechanism of cation permeation in rabbit gallbladder: conductances, the current-voltage relation, the concentration dependence of anion-cation discrimination, and the calcium competition effect. *Journal of Membrane Biology*. 4:331–357.

Wright, E. M., and J. M. Diamond. 1968. Effects of pH and polyvalent cations on the selective permeability of gallbladder epithelium to monovalent ions. *Biochimica et Biophysica Acta*. 163:57–74.